IEEE Access
Multidisciplinary | Rapid Review | Open Access Journal

Date of publication xxxx 00, 0000, date of current version xxxx 00, 0000.

Digital Object Identifier 10.1109/ACCESS.2017.DOI

Joint Power Control and Routing for Rechargeable Wireless Sensor Networks

AMITANGSHU PAL[1], and ASIS NASIPURI[2], (Senior Member, IEEE)
[1]Computer and Information Sciences, Temple University, Philadelphia, PA 19122, USA (e-mail: amitangshu.pal@temple.edu)
[2]Electrical & Computer Engineering, The University of North Carolina at Charlotte, Charlotte, NC 28223, USA (e-mail: anasipur@uncc.edu)

Corresponding author: Amitangshu Pal (e-mail: amitangshu.pal@temple.edu).

"This work was supported by NSF grant CNS-1117790."

ABSTRACT Wireless sensor networks (WSN) that are powered by energy harvested from the environment, also known as rechargeable WSNs, typically experience wide variations of energy availability across the network. Such variations can cause frequent node outages at specific locations where energy availability is low, whereas the remaining nodes may receive sufficient energy for continuous operation. The energy availability also varies over time due to environmental factors, which exacerbates the problem. To minimize the impact of such spatial and temporal variations of energy resources, we propose a joint *Power COntrol and Routing scheme (PCOR)* that adapts the energy consumption in the sensor nodes according to its available energy resources in order to facilitate uninterrupted operations. The scheme is applied to data collecting WSNs with a MAC that utilizes asynchronous duty-cycling for energy conservation. PCOR achieves its objective by reducing the energy consumption at energy-critical sensor nodes, i.e. nodes that have comparatively lower energy resources, using network-wide cooperative power control and route adaptations. This is accomplished by reducing the overhearing at energy-critical nodes, which is a key cause of energy consumption in such networks. We demonstrate through simulations and experimental results that PCOR reduces overhearing at energy-constrained nodes by up to 75% without significantly affecting the end–to–end packet delivery rates.

INDEX TERMS Wireless sensor networks, rechargeable networks, power control, adaptive routing, distributed algorithms.

I. INTRODUCTION

Energy harvesting from environmental resources is a popular approach for achieving long term sustainability in wireless sensor networks (WSN). Although environmental energy harvesting can potentially provide unlimited lifetime, it also introduces unique design challenges for avoiding sporadic node outages. The primary reason is that it is difficult to predict the patterns of ambient energy from environmental resources as well as that of energy usage in the network prior to deployment. For instance, when using solar power harvesting, all nodes experience unpredictable diurnal and seasonal variations of solar irradiance. In addition, the effect of shading from nearby obstructions varies randomly from one node to the next. Similar variations occur with other sources of renewable energy resources as well, such as mechanical energy from vibrations, thermal gradients, and electromagnetic waves, which are gaining increasing interest for powering low power rechargeable devices [1], [2]. The energy consumption also varies significantly and unpredictably from node to node, depending on the sensing, communication, and computation activities at the nodes. A viable approach to avoid node outages under this situation is to develop adaptive networking protocols [3]–[6] to control the energy usage at sensor nodes depending on the state of charge of their rechargeable batteries. In this work, the objective is to develop a mechanism to reduce the energy consumption in nodes that have comparatively lower energy resources at the cost of adaptations of other nodes that are not energy-constrained.

We consider WSNs for environmental monitoring applications, where all nodes periodically transmit their sensor observations to a centralized base station. The sensor nodes communicate over multihop paths that are determined by a dynamic link-quality based routing protocol such as the *Collection Tree Protocol (CTP)* [7]. One of the most effective strategies for conserving energy in WSNs is to utilize sleep

This article has been accepted for publication in a future issue of this journal, but has not been fully edited. Content may change prior to final publication. Citation information: DOI 10.1109/ACCESS.2019.2937894, IEEE Access

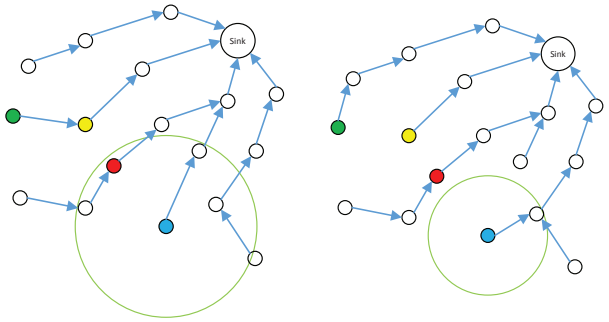

(a) Before adaptations **(b)** After adaptations

FIGURE 1: Illustration of the benefits of power control and route adaptation for reducing overhearing at an energy-constrained node marked in red. Here the black node reduces its transmit power and adapts its route, and the green node adapts its route. All these adaptations reduce the overhearing at the red node.

modes of the transceiver in the sensor nodes whenever possible, which is best implemented using synchronized sleep and wake periods. However, this requires network-wide time synchronization, which increases overhead. The need for time synchronization is avoided by using *asynchronous duty-cycling* of sleep-and-awake cycles of the sensor radios, such as low-power listen (LPL) [8], which is particularly effective for large networks with low network traffic. LPL conserves energy by enabling the receivers to operate under extremely low duty cycles while periodically checking the channel for radio activity. A long preamble is added to each transmitted packet so that receivers do not miss transmissions while going through their periodic sleep and wake cycles. However, excessively long preambles increase overhearing [9], [10] in the network, which is often the critical energy consuming factor in large-scale mesh sensor networks that use asynchronous duty-cycling [11], [12]. Several mechanisms have been proposed to reduce the energy wasted from overhearing, which include interruption of unnecessary receptions based on information transmitted in the preamble [13], adaptive duty-cycling [14], [15] and others. But these mechanisms do not completely eliminate overhearing.

We propose a mechanism to achieve controlled reduction of overhearing at severely energy-constrained nodes to reduce their energy consumption by using cooperative transmission power control as well as through network-wide route adaptations. An illustration of the proposed approach is presented in Fig. 1, where the node marked in red is assumed to have lower energy resources compared to other nodes. It is assumed that routes are initially formed using a route quality metric such as that used in CTP, which disregards energy considerations. These initial routes are illustrated in Fig. 1(a). Note that the red node overhears transmissions from all its neighbors, including the blue and yellow nodes. Also, the yellow node falls in the designated route of the green node, which contributes to its transmission load, and consequently to the overhearing at the red node. The proposed power control and routing approach aims to apply adaptations that would result in a scenario as depicted in Fig. 1(b), which benefits the red node in two ways. First, one of its neighbors (marked in blue) applies transmit power control and route adaptation in order to *avoid* causing overhearing to the red node. A consequence of this adaptation is increasing the route length of the blue node, presumably increasing its end-to-end delay. Second, the green node *switches its route by choosing a different parent*, thereby reducing the traffic at the yellow node, and hence the overhearing caused to the red node. Both of these adaptations reduce the energy consumption at the red node.

Most sensor platforms allow radio transmission at multiple transmit power levels that can be controled dynamically. For example, the CC2420 radio in Crossbow's MicaZ motes [16] provides 32 transmission power levels ranging from -25 dBm to 0 dBm. Dynamic power control for WSNs has been explored significantly in literature, primarily with the objective of reducing interference effects in order to improve the network throughput [17]. A detailed discussion on existing work on power control is presented in the next section.

The primary contributions of the current work are as follows. We target the objective of developing network-wide adaptations that enable rechargeable WSNs to minimize node outages autonomously in the presence of spatio-temporal variations of environmental energy. The proposed scheme achieves this objective by addressing the overhearing problem, on which research has been relatively scarce. We assume that *all nodes* have useful time-sensitive sensor data, i.e. nodes may not be put to sleep for extended periods of time to reduce overhearing. The proposed scheme applies a novel joint power control and routing scheme to reduce overhearing at specific nodes. The distinctive feature of the proposed scheme is that the desired energy conservation of an energy-constrained node is achieved by adaptations of power levels and traffic of its *neighbors*. Consequently, effective overhearing control requires collective cooperation of the neighbors of energy-constrained nodes to help them meet their energy budgets while performing their required sensing and communication tasks.

The proposed tasks also involve maintaining adequate transmission link quality and network connectivity. PCOR addresses these issues by deriving benefits from two approaches. First, in PCOR the sensor nodes apply a prediction model to determine the extent of reduction of their transmit power levels without significantly deteriorating the packet delivery quality to their parents. Secondly, PCOR utilizes a routing metric that combines link quality with additional parameters to capture the overhearing effects caused by the transmissions of the candidate routes that pass through the energy-critical nodes.

The rest of the paper is organized as follows. Section II summarizes related work on power control in wireless networks. In section III, we describe the motivation and background behind our work. Section IV describes the protocol overview of PCOR along with descriptions of some metrics. Section V presents development of an analytical model of link-quality corresponding to different power levels. Section

This article has been accepted for publication in a future issue of this journal, but has not been fully edited. Content may change prior to final publication. Citation information: DOI 10.1109/ACCESS.2019.2937894, IEEE Access

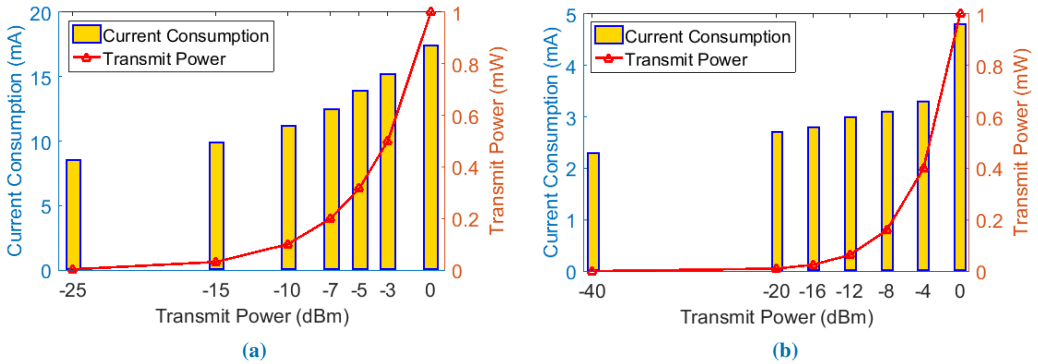

FIGURE 2: Current consumption at different transmit power levels for (a) CC2420 [18] and (b) Nordic nRF52840 radios [19].

VI describes details of the the proposed PCOR protocol. Performance evaluations are discussed in section VII. The paper is concluded in section VIII.

II. RELATED WORKS

Power control has been effectively applied in a wide range of wireless networks for benefits in interference management, energy management, and connectivity management [20]. In cellular networks transmit power control has been primarily applied to mitigate interference and thereby increase the network capacity. Examples include [21], [22] where the authors proposed centralized power control techniques for TDMA/FDMA cellular networks to maximize the minimum signal-to-interference ratio (SIR) of the cellular links. In [23] the authors have extended this for distributed environments. Authors in [24] have developed a power control scheme for CDMA cellular networks. In [25] the authors have proposed a power control scheme in the context of general wireless networks to improve the network capacity. Authors in [26] have proposed a game-theoretic power control scheme in the context of cognitive radio networks. In [27] the authors have used power control scheme in the context of vehicular networks for improving the public safety. Relevant survey articles on power control may be found in [28], [29]. Note that as opposed to cellular networks, wireless interference is relatively of low importance in WSNs due to its small packet sizes and data volume.

A significant amount of work has also been reported on transmission power control approaches for low-power networks such as WSNs. Key considerations include topology control, where a desirable property such as K-connectivity is preserved while applying power control in dense wireless networks [30]–[33]; power aware routing, where routes (and possibly corresponding transmission levels) are chosen based on residual energy levels at the nodes [34]–[37]; and sleep management, where a subset of wireless nodes are turned off to conserve energy [38]–[40]. More recently, in cognitive radio networks [41], power control is also associated with pricing issues. A large volume of this work includes application of game-theoretic approaches [42]–[44].

The contributions of [45]–[49] are to find the number of neighbors of each node and adjust their radio transmission powers so that the number of neighbors stays within a desired range. In [45], the authors propose a power control scheme where a node maintains a list of neighbors whose signal strength are higher than some threshold, and it adjusts the radio transmission power if the number of neighbors is outside the predetermined bound. Authors in [46] propose a similar scheme where a node determines its range by counting the number of nodes that acknowledge to its beacon messages. In [47], the authors propose a scheme where each node ranks neighboring nodes in the order of their signal strengths and adjusts their radio transmission power so that it covers only a minimum number of neighbors with reasonable signal strength. A similar power control scheme is described in [50] where a node adjusts its transmit power to keep the number of neighbors within a predefined value to ensure network connectivity. Authors in [51] have developed a real-time power aware routing (RPAR) where specific network parameters such as communication delays or packet deadlines are crucial. In PCBL scheme [48], each sensor node sends some packets with different power levels to measure the quality of the link. It then adjusts its radio transmission power for each destination node with the smallest possible value such that a minimum packet reception ratio is achieved. The scheme also filters out the nodes that have extremely low reception ratios. In ATPC [49], the authors propose a feedback-based transmission power control scheme that dynamically measures link qualities over time. Each node broadcasts beacons at different transmission power levels, and its neighbors measure signal strength and a link-quality indicator corresponding to these beacons and send these values back by a notification packet. After the notification packet is received, the beaconing node determines the optimal transmission power level individually for each neighbor. Another control theory based transmission power control scheme is proposed in [52] where the authors design a dynamic control model that combines a theoretical link model with online parameter estimation. These contributions are mostly motivated by link quality and performance considerations such as increasing network capacity.

This article has been accepted for publication in a future issue of this journal, but has not been fully edited. Content may change prior to final publication. Citation information: DOI 10.1109/ACCESS.2019.2937894, IEEE Access

(a) Oil-filled circuit breakers **(b)** Oil-cooled transformers

FIGURE 3: Illustrations of wireless sensor nodes deployed in *ParadiseNet*: (a) locations of surface temperature sensor nodes, and (b) temperature, vibration, and sound intensity sensor nodes.

As opposed to the contributions mentioned above, here we apply power control for energy management with the ultimate objective of reducing outages in rechargeable wireless sensor nodes. The existing literature on energy management exploits the benefits of power adaptation by dropping the power levels of a transmitter so that the signal strength at the receiver is just above the receiver sensitivity. While this helps in reducing the energy consumption in high power wireless transmitters such as cellular and ad hoc networks, in low-power radios such as those used in WSNs, it does not lead to *proportional reduction in power consumption* of the transmitter. This is due to the fact that the baseline operations of low-power transceivers are already optimized for very low power consumption [53]. Moreover, low-power radios have a high overhead of power consumption from its active circuit elements such as oscillators and active mixers, which can consume up to a few hundreds of microwatts. Fig. 2 depicts the power consumption data obtained from two commercial radios that are typically used in WSNs, which indicate that these low power radios do not achieve proportional energy savings by dropping the power levels at the transmitters. For example CC2420 radios consume 17.4 mA while transmitting at 0 dBm transmit power and 8.5 mA at -25 dBm transmit power [18], i.e. a 50% reduction in current consumption for a three orders of reduction in transmit power level. On the other hand, a Nordic nRF52840 chip draws 4.8 mA at 0 dBm and 2.3 mA at -40 dBm [19], i.e. to achieve a 50% reduction in current consumption, the radio sacrifices a four orders of magnitude reduction in transmit power levels.

In contrast, PCOR achieves energy savings by utilizing the fact that decreasing the transmit power at a transmitter reduces the current consumption of its *neighbors* by reducing their overhearing. In particular, PCOR applies transmit power control to neighbors of energy critical nodes so as to conserve their valuable energy resources. In addition, PCOR adapts routes so that the overall network traffic is reduced at regions near critically energy constrained nodes. This is achieved not solely by power adaptation, but with joint power adaptation and network-wide route adaptation as explained in Fig. 1. To the best of our knowledge, PCOR is the first work that tries to alleviate the overhearing effects on energy–critical nodes through joint network wide power and route adaptations.

III. MOTIVATION AND BACKGROUND

This work is driven by experiences from a real-life WSN testbed that was developed by the authors for real time condition monitoring of high-power equipment in a TVA-operated power substation in Kentucky (see Fig. 3). The project, sponsored by EPRI, resulted in the deployment of a 122-node WSN known as *ParadiseNet* in a 1000×400 feet area in the power substation to detect early signs of potential failure conditions from equipment such as circuit-breakers and transformers. The wireless sensors were developed using Crossbow's (currently MEMSIC) MICAz motes that used a low power mesh networking protocol called *XMesh* [54] for forwarding periodic sensor observations to a base-station. *XMesh* applies a quality aware routing metric, which does not incorporate energy-awareness. Low-power (LP) operation is achieved by LPL, where nodes remain in sleep modes as long as possible, wake up for brief periods of time to detect possible radio activity and then remain awake if an activity is detected. As stated earlier, asynchronous transmissions using LPL does not eliminate *overhearing*, which varies considerably across different nodes in a randomly deployed WSN. Illustrations of deployed wireless sensor nodes in ParadiseNet are depicted in Fig. 4(a). Out of these, 15 nodes were solar energy harvesting nodes that were developed using Heliomotes from Alta Labs [55] and deployed at select locations to measure solar irradiance characteristics. The rest were powered by 3V 5000mAH Lithium batteries, which were used to measure energy usage characteristics from voltage drop observations. Results from the testbed highlight the following two features that impact reliable long-term operation of the WSN for network-wide condition monitoring.

Non-uniform current consumption: Fig. 4(b) depicts the distribution of the drops in the battery levels in different nodes with fixed (non-rechargeable) batteries over a period of five months of operation, which indicates a wide variation of battery usage in different nodes. Fig. 4(c) illustrates the average battery voltage drops of the sensor nodes in four

This article has been accepted for publication in a future issue of this journal, but has not been fully edited. Content may change prior to final publication. Citation information: DOI 10.1109/ACCESS.2019.2937894, IEEE Access

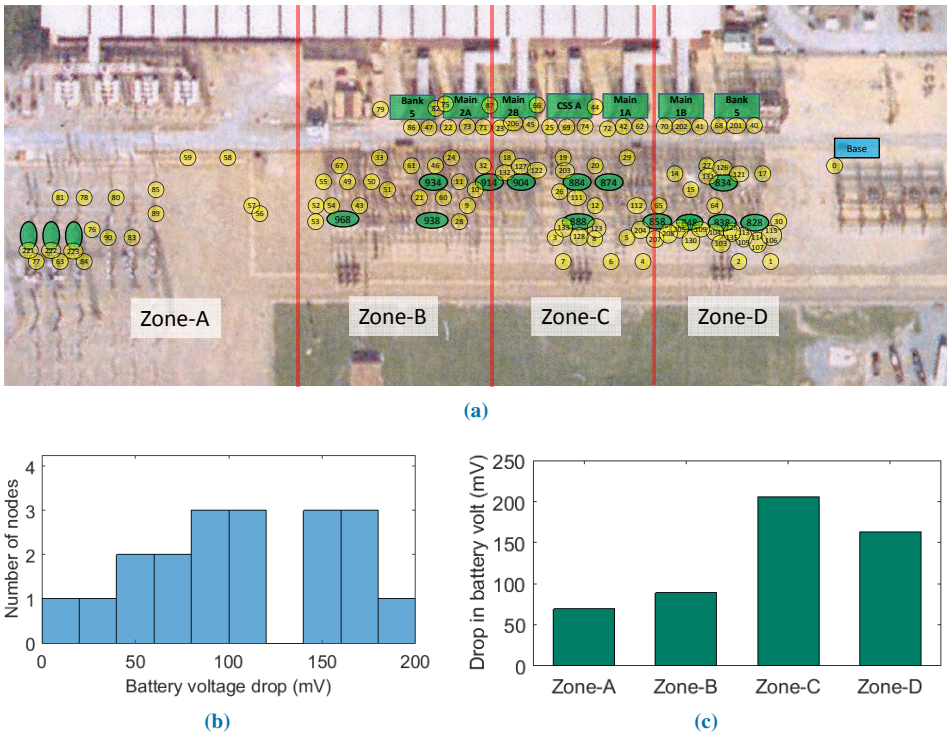

FIGURE 4: (a) Deployment map of *ParadiseNet*, which consists of the 122 WSN nodes deployed in TVA's Paradise substation. (b) Histogram of voltage drops and (c) average drop of battery voltage in each of the zones in ParadisNet over a period of five months.

zones of the network that are shown in Fig. 4(a), which indicates that the nodes closer to the base station, i.e. Zone-C and D, have higher voltage drops than the other two zones. The nodes in Zone-C experience the highest drop, potentially due to heavier traffic and overhearing. This imbalance leads to uncontrolled energy consumption of some nodes in the network, which ultimately results in energy depletion of few nodes dying earlier than others. This will collectively result in network partitioning and thus decrease in connectivity, performance and overall lifetime of the network.

Spatio-temporal variation of energy availability: The field results presented in Fig. 5 highlight several of the major issues with solar power harvesting. Firstly, ambient energy sources such as sunlight tend to be time-dependent and non-stationary. This is illustrated in Fig. 5(a), which shows how global horizontal radiation typically varies over the course of a year [56]. Note that there are clear peaks and valleys that match seasonal patterns. In addition, there are significant day-to-day variations resulting from cloud cover, air quality, and other environmental effects. These natural variations are not the only factors affecting the source profiles of individual nodes. Fig. 5(b) demonstrates, for instance, the strong local variations resulting from the different shading patterns at two different nodes. While node 84 experiences high irradiation levels in most days, node 70 gets very few days when the average irradiation is > 400 W/m^2 (the *Heliomotes* were found to charge when irradiation >250 W/m^2). To illustrate such spatial variations of harvested energy availability, we plot the distribution of average irradiance measurements from the 15 solar harvesting nodes in ParadiseNet in Fig. 5(c). The results were taken in between 7 am and 7 pm on a sunny day of 14th April, 2010. From this figure we can observe that almost 90% of the nodes have an average irradiance less than 500 W/m^2, whereas 40% nodes have an irradiance level below 300 W/m^2.

An additional problem is that uncertainty is not unique to the source profile. Energy-storage elements are also affected by various external factors. This is clearly seen in Fig. 5(d), which shows how battery voltage varies with ambient temperature. Fig. 5(e) depicts the variations of the battery voltage of a solar-powered node (capped at 2.5V due to limitations of the ADC) as obtained from packets received from it. The gaps in transmission are caused by node outages that occur when the battery voltage drops below the lowest allowable input for the dc-to-dc converter, which is 2.2V. These outages are more frequent from February – April, when the radiation levels are comparatively lower.

These indicate that high temporal and spatial variations of solar energy pose major design challenges for achieving uninterrupted operations of the solar-powered sensor nodes. Even if a more effective energy harvesting solution than the *Heliomote* is used, the inherent variability of the renewable energy source warrants the need for a solution that enables the nodes to adapt to these variations while maintaining continuity of operations.

IV. PRELIMINARIES AND PROTOCOL OVERVIEW

In this section, we explain the proposed approach for

This article has been accepted for publication in a future issue of this journal, but has not been fully edited. Content may change prior to final publication. Citation information: DOI 10.1109/ACCESS.2019.2937894, IEEE Access

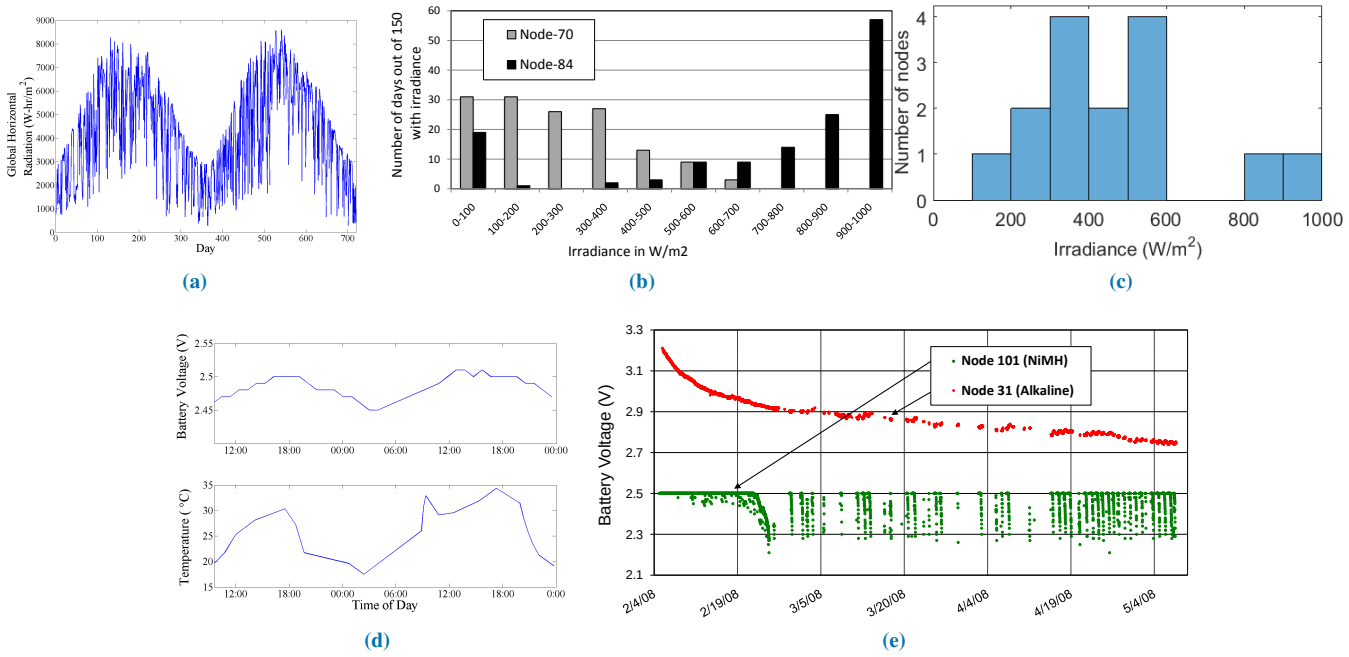

FIGURE 5: Challenges affecting the design of solar power harvesting nodes: (a) Total daily global horizontal radiation in Nashville, TN, between January 1, 1989 and December 31, 1990. (b) Histograms of the average irradiance received per day at node-70 and node-84 from *ParadiseNet* over a period of five months, and (c) Distribution of irradiance measurements across the nodes in ParadiseNet. (d) Temperature dependence of battery voltage in a wireless sensor node installed in *ParadiseNet*. (e) Battery voltage variations in a solar power harvesting node (node 101) demonstrating frequent outages.

network-wide transmission power control and route adaptations to enable the nodes to adapt to such spatio-temporal energy variations. As stated in section II, we apply transmission power control to achieve energy savings by reducing *overhearing*. This benefit, however, is achieved at listening nodes and not at the transmitter. Note that overhearing can also be eliminated by applying scheduling schemes [57]–[60], where nodes maintain non-overlapping transmission schedules. However, that requires time-synchronization among the nodes, which can be challenging to achieve in large-scale networks, and hence we do not consider that in this work.

To estimate the potential energy savings of applying power control, we consider an example scenario as shown in Fig. 6(a) and calculate the key components of the energy consumption in the network for a multi-hop transmission from S to D under various transmission powers. Assuming that power control is ideal where all nodes adapt their transmission range R to the desired hop length d/h, the total energy consumed in the network for this transmission can be expressed as:

$$E_{\text{total}} = hE_{\text{tx}} + h\rho A_R E_{\text{rx}} + E_{\text{other}} \quad (1)$$

where $E_{\text{tx}} = E_{\text{radio}} + E_{\text{elec}}$ is the total energy spent in transmitting a packet, E_{radio} is the part of the energy spent in the radio transmitter, E_{elec} is that spent in the electronics, ρ is the node density, $A_R = \pi R^2$ is the expected area around a transmitting node where the packet is received by other nodes assuming isotropic propagation, E_{rx} is the total energy spent in receiving packets and is largely attributed to overhearing, and E_{other} represents the total energy spent in the node in performing all other activities during this period of time (such as processor, ADC, radio idle time, etc.). Note that with ideal power control, $E_{\text{radio}} = E_{\text{Tmax}}(R/d)^{\alpha}$ where E_{Tmax} is the energy spent in the transmitter for transmitting to its maximum distance (i.e. $R = d$) and α is the path loss exponent. Fig. 6(b) depicts the variations of the different energy components with h. The results show that while the energy consumed in transmissions and electronics increase with h, the energy consumed in receptions, which is the key component affecting the total energy consumed in the network, reduces with increasing values of h, i.e. shorter transmission ranges. Hence, in a scenario where all nodes are communicating to D, the average energy consumption per node will be minimum when all nodes transmit at the lowest possible power level[1]. The energy savings will be more prominent at a higher node density, which is a key motivation for applying power control in large-scale WSNs [9].

In PCOR, the neighbors of an *energy-critical node* cooperatively reduce their transmit power to avoid causing overhearing on the critical node while maintaining connectivity and/or link quality. This results in a multi-variable optimization problem that connects several issues in addition to average energy consumption, including transmission link quality and network connectivity. PCOR applies a *statistical prediction*

[1]These results were computed using representative parameters of low-power wireless sensor nodes, such as *MICAz*. The results will look somehwat different when computed for high-power wireless devices where the energy usage for RF transmissions dominate over that used for receiving and electronics.

This article has been accepted for publication in a future issue of this journal, but has not been fully edited. Content may change prior to final publication. Citation information: DOI 10.1109/ACCESS.2019.2937894, IEEE Access

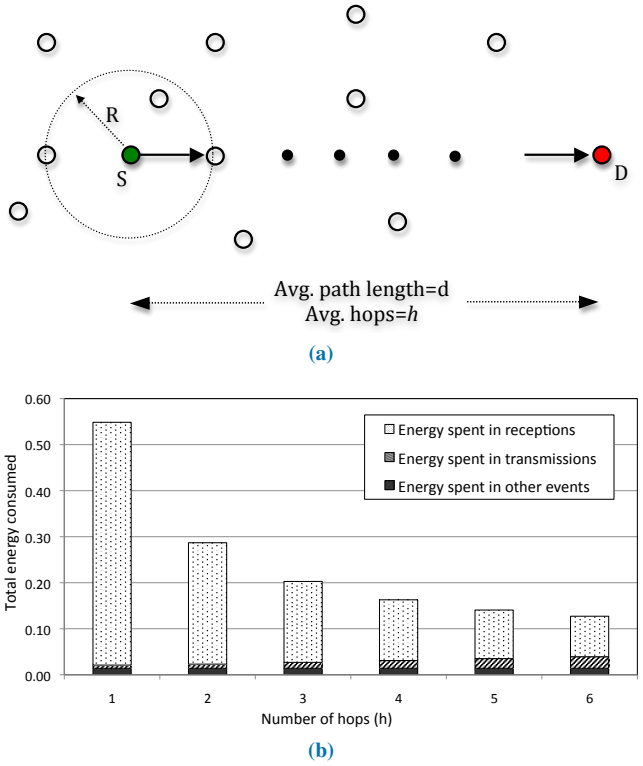

FIGURE 6: Illustration of dependence of total energy consumed on the number of hops for a multihop route. The idealized model is illustrated in (a), and the variation of the total energy consumed for a multihop packet transmission from S to D is illustrated in (b).

model to (i) measure the extent by which a node can reduce its transmit power while maintaining a reasonable link quality to its parent and (ii) the amount of overhearing caused to energy-critical nodes, which we discuss in section IV. Before going into the details on the proposed scheme in section V, we discuss some related terminologies and definitions first. The necessary notations are depicted in Table 1.

A. HEALTH METRIC AND BATTERY CAPACITY MEASUREMENT

The mechanism applied by a sensor node to measure its battery health, current consumption and battery capacity in PCOR is described below.

Definition 1 (Battery health-metric): We define the *battery health-metric* H of a node by its remaining battery lifetime under the currently estimated power consumption. Thus H of a node is the estimated time until its battery is depleted under the current power usage. We assume $H = \frac{B}{\mathcal{I}}$, where B is the remaining battery capacity of the node and $\mathcal{I}$ represents its estimated current consumption.

The current consumption of a sensor node is given by:

$$\begin{aligned}\mathcal{I} &= \frac{I_{Bt}T_{Bt}}{T_B} + M.I_{Dt}T_{Dt} + N.\frac{I_{Br}T_{Br}}{T_B} + O.I_{Dr}T_{Dr} \\ &+ F.I_{Dt}T_{Dt} + \frac{I_S T_S}{T_D} + \eta_P.I_P T_P \end{aligned} \quad (2)$$

where the current consumption and time duration due to different tasks are mentioned in Table 1. The beacons and data packets are transmitted with an interval of T_B and T_D respectively. We assume that the overhearing and forwarding rates of the sensor nodes are denoted by O and F respectively. N is the number of neighbors of the sensor node. M is the rate at which a sensor node transmits its own packets. If there are no retransmissions, then $M = \frac{1}{T_D}$. We assume that the sensor node uses LPL, where it wakes up η_P times in a second to check whether the channel is busy or not, which we define as *processing* task. If the channel is idle it goes back to sleep, otherwise it stays on till the end of the ongoing transmission. In our application we set η_P to 8. We assume that the nodes can estimate the dynamic parameters used in (2), by periodic assessments of its overheard and forwarded traffic.

We consider a time-domain approach for estimating the battery capacity B, which was developed as part of the *ParadiseNet* project. The details of this method are beyond the scope of this paper. In this approach, a small test signal is superimposed on top of the battery load. This triggers a transient dynamics. We measure the terminal voltage and current, and then the impedance parameters of the battery model is estimated using a nonlinear least-squares routine. These parameter values are then used to estimate B over time.

Definition 2 (Energy-critical node): A node is defined as energy-critical if its health-metric is *less than some fraction of the health-metrics of its neighboring nodes*. Formally a node is critical if its $H < \alpha.\mu_H$, where μ_H is the mean of its neighbors health metrics. α is a fraction which is less then 1.

The nodes carry a field in their beacon messages, named *critical node (CN)* to define the energy-critical state of a node; where $CN = 1$ implies that the node is energy critical, and $CN = 0$ otherwise.

Definition 3 (Probability of control or POC): The beacon messages also carries another field called the *probability of control (POC)* to represent the extent to which a node requires adaptation based on its battery health in comparison to the average battery health of neighboring nodes. For an energy-critical node, $POC = \frac{\mu_H - H}{\mu_H}$. For all other nodes that are not energy-critical $POC = 0$.

An energy-critical node uses the parameter POC to indicate how aggressively its neighbors need to adapt their transmit power levels. A high value of POC indicates that the node is extremely critical, thus prompting its neighbors to reduce their transmit powers with high probability. A POC = 0 implies that no power control is needed.

B. ROUTING METRICS

In addition to the energy considerations of the critical nodes, PCOR also ensures a certain desired quality of the established routes. To estimate the quality of a route, we define a path metric which is the sum of the *expected number of attempts required for successful transmission (ETX)* on each of its links. The same principle is used in the CTP. We first define different routing metrics as follows:

This article has been accepted for publication in a future issue of this journal, but has not been fully edited. Content may change prior to final publication. Citation information: DOI 10.1109/ACCESS.2019.2937894, IEEE Access

Definition 4 (ETX of a link or link-ETX): An ETX of a link is the expected number of transmission attempts required to deliver a packet successfully over the link. The link-ETX of the link $i \rightarrow j$ is denoted as ℓ_{ij}.

Definition 5 (ETX of a path or path-ETX): An ETX of a path is the sum of the link-ETXs of all the links along the path. Assume that Ω_i is the neighbor set of node i. Then node i has atmost $|\Omega_i|$ routes to the sink, each one goes through a neighbor $j \in \Omega_i$. We define the path-ETX of the route from i that hops through j as $\wp_{ij}$.

Definition 6 (ETX of a node or node-ETX): Each node calculates its ETX as the ETX of its *parent* plus the ETX of the link to its parent, i.e. the path-ETX of the route that hops through its parent. We define the ETX of node i as ζ_i. In CTP the parent is selected as follows. The sink always broadcasts an ETX = 0. The node i chooses node $j \in \Omega_i$ as its parent among all its neighbors if

$$\ell_{ij} + \zeta_j < \ell_{ik} + \zeta_k \quad \forall k \neq j \in \Omega_i \tag{3}$$

In this process a node chooses the route with the lowest path-ETX to the sink.

Definition 7 (min-ETX): We define min-ETX of a node as the path-ETX of the best quality route towards the sink. min-ETX of node i is denoted as λ_i. Notice that in CTP $\lambda_i = \zeta_i$. However in PCOR this is not the case, as the nodes choose the route that reduces overhearing n the critical nodes as opposed to always choose the best quality route to the sink.

TABLE 1: Table of Notations

$I_{Bt}/I_{Dt}/I_{Br}$ $/I_{Dr}/I_S/I_P$	$\triangleq$	Current consumption due to beacon transmission/data transmission/beacon reception/data reception/sensing/processing
$T_{Bt}/T_{Dt}/T_{Br}$ $/T_{Dr}/T_S/T_P$	$\triangleq$	Time duration for beacon transmission/data transmission/beacon reception/data reception/sensing/processing
$\mathcal{T}_{ov}^i$	$\triangleq$	Total overhearing caused by node i and its route, on the critical nodes, due to its forwarding traffic to the sink
$\mathcal{L}_{ov}^{ij}$	$\triangleq$	Total overhearing caused by i and its route, on the critical nodes, if it chooses j as its parent
p_{ov}^{ij}	$\triangleq$	Probability that the worst critical neighbor of i overhears a packet transmission by link $i \rightarrow j$ corresponding to the transmit power t_{ij}
$\mathcal{E}^m$	$\triangleq$	Minimum link-ETX threshold to start power reduction
$\mathcal{E}^M$	$\triangleq$	Threshold beyond which a node starts increase its power
$\ell_{ij}/\wp_{ij}$	$\triangleq$	link-ETX/path-ETX of $i \rightarrow j$
ζ_i/λ_i	$\triangleq$	node-ETX/min-ETX of i
t_{ij}	$\triangleq$	Transmit power of i required to achieve a minimum link quality of link $i \rightarrow j$ from the prediction model
t_c/t_i	$\triangleq$	Current/i-th transmit power of a node
Ω_i	$\triangleq$	Set of neighboring nodes of i

V. PREDICTION MODEL FOR POWER CONTROL

Since the link quality between a pair of nodes largely depends on the transmit power level of the transmitter, we develop a *receiver-based* prediction model *to correlate the transmit power level at the transmitter and forward link quality at the receiver.* By using the *log-normal shadowing* model, the *packet delivery ratio (PDR)* of a link can be modeled as

$$\begin{aligned} PDR &= \text{Prob}\left[P_r(d) > \gamma\right] = \text{Prob}\left[P_t - P_l(d) > \gamma\right] \\ &= \text{Prob}\left[P_t - \overline{P_l(d)} + X_\sigma > \gamma\right] \\ &= Q\left(\frac{\gamma - P_t + \overline{P_l(d)}}{\sigma}\right) \end{aligned} \tag{4}$$

where it is assumed that the link distance is d, $P_r(d)$ and $P_l(d)$ are the power received and path loss at the receiver end, P_t is the transmit power level, and γ is the desired receiver signal threshold. X_σ is a zero-mean Gaussian random variable with standard deviation of σ. X_σ mainly models the shadowing effects which results in due to the fading and environmental noise, which causes small-scale signal fluctuation at the receiver end.

Using (4) we develop a measurement-based *online* prediction model that approximates a function to represent a relationship between the packet delivery ratio p and the transmit power t. The function is adapted over time to reflect the temporal changes. To model the function corresponding to a test link, let us assume that the transmitter sent a group of data packets at N power levels $\mathbb{T} = \{t_1, t_2, ..., t_N\}$ and the corresponding delivery ratios are found to be $\mathcal{P} = \{p_1, p_2, ..., p_N\}$. From (4) we can observe that the distribution of delivery ratios at different transmit power levels follows an *error function* which can be approximated as a sigmoid function. Thus the relationship between $\mathbb{T}$ and $\mathcal{P}$ can be approximated as

$$p_i = \frac{1}{1+e^{-(a.t_i+b)}} \quad \Rightarrow a.t_i + b = \ln\left(\frac{p_i}{1-p_i}\right) = P_i \text{ (say)} \tag{5}$$

Fig. 7 shows the experimental validation of a set of sigmoid curves that represent this model. In Fig. 7 we place a pair of MICAz motes in 4 different places and the packet delivery ratios at the receiver at different transmit power levels.

To formulate the predictive model we use two vectors $\mathbb{T}$ and $\mathbb{P}$, where $\mathbb{P} = \{P_1, P_2, ..., P_N\}$. Expressing (5) in matrix

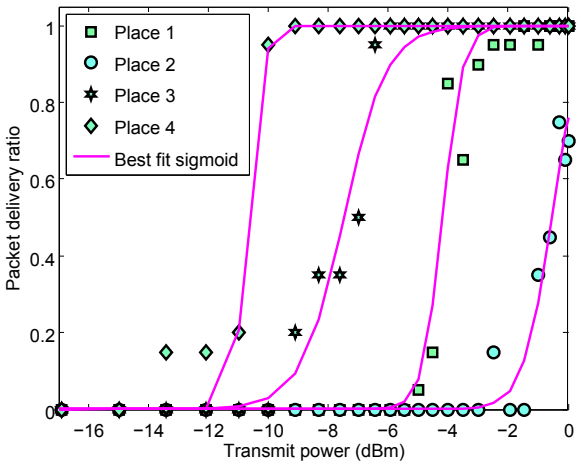

FIGURE 7: Illustration of the packet delivery ratio vs transmit power.

This article has been accepted for publication in a future issue of this journal, but has not been fully edited. Content may change prior to final publication. Citation information: DOI 10.1109/ACCESS.2019.2937894, IEEE Access

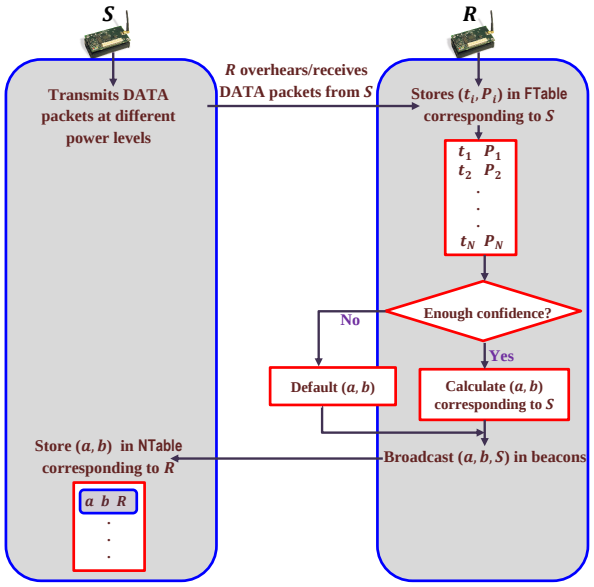

FIGURE 8: Receiver-oriented prediction model.

form we get

$$\begin{bmatrix} t_1 & 1 \\ \vdots & \vdots \\ t_N & 1 \end{bmatrix} \begin{bmatrix} a \\ b \end{bmatrix} = \begin{bmatrix} P_1 \\ \vdots \\ P_N \end{bmatrix}$$

$$\Rightarrow \begin{cases} a = \dfrac{\sum P_i . \sum t_i - m . \sum t_i . P_i}{\sum t_i . \sum t_i - m . \sum t_i^2} \\ \text{and} \\ b = \dfrac{\sum P_i - a . \sum t_i}{m} \end{cases} \tag{6}$$

where the *coefficients* a and b are calculated using a linear regression curve-fitting approach. Due to the temporal fluctuations, the t_i and P_i values changes and thus the values of a and b can be updated too. These parameters are calculated at the receiver end and broadcast using beacon messages, so that the transmitter can record those values. Notice that *the beacon messages are sent using the highest power so that all neighboring nodes can receive them.*

In reality, the receiver accumulates the (t_i, P_i) pairs as follows. The transmitters append their current transmit power levels (of their data packets[2]) in their beacon messages. The data packets carry a sequence number so that the receivers (or overhearers) can track them and calculate the packet delivery ratio (or link-ETX) corresponding to any power level. The receivers *opportunistically* record (through reception or overhearing) the transmit power and packet delivery ratio corresponding to each transmitters, in a table called *Feedback Table* (or `FTable`). For each neighbor $i \in \Omega_j$, the `FTable` contains the following fields: ⟨nodeID of i, power-level of i, PDR of $i \rightarrow j$, link-ETX of $i \rightarrow j$, a, b⟩. When a receiver gets enough confidence over a link, i.e. it accumulates enough `FTable` entries covering a wide range of delivery ratio and transmit power levels, it runs the prediction model and records the (a, b) pair. When j transmits beacon messages, it appends the nodeIDs along with their corresponding to the (a, b) pair from the `FTable`. The accuracy of this model is further improved with more number of (t_i, P_i) samples. Before it accumulates enough samples (or confidence) to run this model corresponding to a transmitter, it simply broadcasts a and b with their default values.

The transmitter i then uses the (a, b) pair to estimate the link quality of $i \rightarrow j$ at any power level from (4)-(5). The transmitter i also maintains a table called Neighbor Table (or `NTable`). For each neighbor $j \in \Omega_i$ the `NTable` stores the following fields: ⟨nodeID of j, PDR of $i \rightarrow j$, link-ETX of $i \rightarrow j$, node-ETX of j, a, b⟩. The `NTable` is used for calculating the transmit power levels and routers as described in section VI. The overall scheme is depicted in Fig. 8.

Notice that in this scheme a node j appends the nodeIDs of its neighbors (i.e. $\forall i \in \Omega_j$) and their corresponding coefficients in their beacon messages, which may increase packet size. To restrict the packet size, the nodeIDs and the coefficients are appended in a round-robin fashion, each time with n neighbors. In our experiments, we assume $n = 3$.

This prediction model is used by the nodes for two purposes. First, using this model a node can decide how much power it can reduce corresponding to a receiver while maintaining a certain link quality. Second, the node can also calculate that with certain transmit power level, what level of overhearing is caused to the energy critical neighbors. Notice that overhearing is typically a physical layer phenomenon; however the amount of overhearing can be approximated by calculating the number of packets received at the network layer.

VI. THE PROPOSED COOPERATIVE JOINT POWER CONTROL AND ROUTE ADAPTATION (PCOR) SCHEME

We now present the joint power control and route adaptation scheme that fulfills two key objectives. First, it reduces overhearing on *energy-critical nodes*. Second, routes are adapted dynamically and in a distributed fashion so that the network traffic reduced at the neighboring regions of the energy-critical nodes. These two mechanisms reduce the energy consumption of critical nodes by reducing their forwarding and overhearing rates. A simplified flow graph of the proposed scheme is depicted in Fig. 9 and the details are explained below.

We assume that each node j exchanges periodic beacon messages with its neighbors $i \in \Omega_j$. The beacon messages include its node ID, its node-ETX value, CN (which is 1 if a node is critical and 0 otherwise), POC, and its current transmit power level. In addition to that, a beacon message also includes the nodeIDs of n neighbors, their corresponding coefficients and the link-ETXs

[2]Notice the difference between the data packets (which carry the sensed values) and beacon messages. While calculating the ETXs (or delivery ratios) the performance of the data packers are only used. Power control is applied only to the data packets and not for the beacon messages. The beacon messages are transmitted periodically and just after any change in transmit power, so that the neighbors can infer that the following data packets are transmitted with new power levels.

This article has been accepted for publication in a future issue of this journal, but has not been fully edited. Content may change prior to final publication. Citation information: DOI 10.1109/ACCESS.2019.2937894, IEEE Access

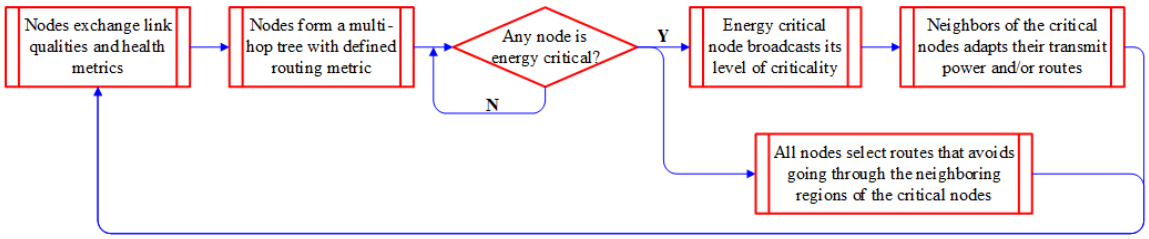

FIGURE 9: Block schematic of the proposed cooperative joint power control and route adaptation scheme, PCOR.

of the links $i \rightarrow j$ or ℓ_{ij}. For the sake of clarity, we describe the transmit power control and parent selection separately in section VI-A and VI-B respectively. The two modules are denoted as `ParentSelectionModule` and `PowerControlModule` respectively in Algorithm 1.

A. POWER CONTROL

If there are no energy-critical nodes in the network, then PCOR works identical to CTP. Each node periodically selects the neighbor that gives the route with lowest path-ETX as its parent. The power adaptation does not take place in this case.

The adaptation process starts when one or more nodes become energy-critical. An energy-critical node broadcasts beacon messages with CN = 1 along with its POC. All its neighbors that receives beacon messages with CN = 1 reduce their transmit power levels if the following conditions are satisfied:

(a) the link-ETX corresponding to its parent is less than some threshold $\mathcal{E}^m$
(b) the current transmit power t_c is more than a minimum threshold ξ

Conditions(a)-(b) ensure that the overall network quality is not compromised due to the power reduction. Each of the neighbors of a critical node then checks whether the (a, b) pair corresponding to its parent in the `NTable` contains their default values or not.

1) Reduce transmit power in steps

If the (a, b) pair corresponding to its parent entry is in their default values, it then reduces its transmit power in steps with a step-size of β, with a probability κ equal to the POC of its critical neighbor (line 20-21 in Algorithm 1). If a node is a direct neighbor of multiple critical nodes, then κ equals to the maximum of all the POCs of its critical neighbors (which is its *worst* critical neighbor). This results in reduced overhearing on the critical nodes.

2) Reduce transmit power using the prediction model

If a neighbor of the critical node finds a non-default (a, b) values in its `NTable` corresponding to its parent, it uses the prediction model to reduce its transmit power (line 22-23 in Algorithm 1). In this case the node uses the minimum transmit power level t to achieve a desired link-quality or PDR which is more than some threshold Υ. Formally

$$t = \left\lceil \frac{\Upsilon - b}{a} \right\rceil \tag{7}$$

where $\lceil x \rceil$ is the next available power level more than x provided by the radio.

Algorithm 1: Proposed power control and route adaptation scheme at node i

1 **Function** `ParentSelectionModule`(i)**:**
2 Γ_i = NULL; ▷ Initialize empty list Γ_i
3 **foreach** *entry j in* `NTable` **do**
4 **if** *((a, b) pair corresponding to j is in default value) $\vee$ (i has no critical neighbor)* **then**
5 Calculate p_{ov}^{ij}, ℓ_{ij} and $\wp_{ij}$ corresponding to t_c;
6 **else if** *((a, b) pair corresponding to j is in non-default value) $\wedge$ (i has some critical neighbors)* **then**
7 Calculate the minimum transmit power t_{ij} to achieve a desired link-quality Υ for $i \rightarrow j$;
8 Calculate p_{ov}^{ij}, ℓ_{ij} and $\wp_{ij}$ corresponding to t_{ij};
9 $\mathcal{L}_{ov}^{ij} = \mathcal{T}_{ov}^{j} + p_{ov}^{ij}$;
10 **if** $(\zeta_i < \zeta_j) \wedge (\ell_{ij} < \frac{1}{\Upsilon}) \wedge (\wp_{ij} < \tau + \lambda_i)$ **then**
11 $\Gamma_i = \Gamma_i \cup j$; ▷ Add j to Γ_i
12 $\mathcal{T}_{ov}^{i} = \min_{\forall j \in \Gamma_i} \mathcal{L}_{ov}^{ij}$; ▷ Calculate TOV of i
13 $l = \arg\min_{\forall j \in \Gamma_i} \mathcal{L}_{ov}^{ij}$; ▷ l becomes the parent of i
14 Call `PowerControlModule`(i, l) if i has any critical neighbor;
15 return l and $\mathcal{T}_{ov}^{i}$; ▷ Return the parent and TOV

16 **Function** `PowerControlModule`(i, l)**:**
17 κ = POC of the worst critical neighbor;
18 **if** $(\ell_{il} > \mathcal{E}^M) \vee (\mathbb{R}$ *consecutive transmissions fail)* **then**
19 $t_{il} = t_{il} + \beta$; ▷ Increase power
20 **else if** *((a, b) corresponding to node l in* `NTable` *is in default value)* $\wedge$ $(\ell_{il} < \mathcal{E}^m)$ **then**
21 $t_{il} = \min\{\xi, t_{il} - \beta\}$ with probability κ; ▷ Decrease power in steps
22 **else**
23 $t_{il} = \min\left\{\xi, \left\lceil \frac{\Upsilon - b}{a} \right\rceil\right\}$ with probability κ using (a, b) corresponding to l in `NTable`; ▷ Decrease power using prediction model
24 return t_{il}; ▷ Return the transmit power level

Note that, if *any* if the following conditions are satisfied (line 18-19 in Algorithm 1), a node starts increasing its transmit power in steps of β to maintain adequate link quality:

(A) the link-ETX to its parent is more than a threshold $\mathcal{E}^M$
(B) its $\mathbb{R}$ consecutive transmissions to its parent fail

For our performance evaluations, we assume $\mathbb{R}$ to be 10.

This article has been accepted for publication in a future issue of this journal, but has not been fully edited. Content may change prior to final publication. Citation information: DOI 10.1109/ACCESS.2019.2937894, IEEE Access

B. PARENT SELECTION

As the change in transmit power level affects the ETX, adapting transmit power may eventually require a node to adapt its route, i.e. parent selection as well. This is shown by the blue node in Fig. 1. Hence, PCOR effectively *ties route adaptations with power control*. On the other hand if a node is not a direct neighbor of a critical node, it does not adapt its transmit power; but it may still select a parent such that the chosen route avoids going through the neighboring regions of the critical nodes (as shown by the green node in Fig. 1). This ensures a *network-wide route adaptations as opposed to independent adaptations just by the neighboring nodes of the energy-critical nodes*. In PCOR we implement such adaptations by the following *route metric*:

Definition 8 (Total Overhearing or TOV): TOV of a node is the measure of overhearing caused by a node's transmission to all energy-critical nodes. Thus TOV of a node i, which is denoted as $\mathcal{T}_{ov}^{i}$, is the total overhearing caused by a transmission from i to any energy-critical nodes in its neighborhood or by one or more of its upstream nodes (i.e. from i to the sink) to energy-critical nodes in their neighborhood.

Before going into the calculation of TOV of a node, we present the following definitions.

Definition 9 (Probability of Overhearing or POV): Assume that Ω_i denotes the neighbor set of i, and $j \in \Omega_i$ is a neighbor of i. Then POV of a link $i \rightarrow j$, denoted as p_{ov}^{ij}, is the probability that a packet transmitted by i (if it chooses j as its parent) is overheard by its *worst energy-critical neighbor* (assume k). POV is basically the packet delivery ratio which can be measured

(1) from the prediction model corresponding to any power level, if the `NTable` entry corresponding to k contains non-default (a, b) pair, or
(2) by taking the inverse of the link-ETX of $i \rightarrow k$ (i.e. ℓ_{ik}) if the coefficients (a, b) are at their default values.

Definition 10 (link-TOV or LOV): The link-TOV of a link $i \rightarrow j$, denoted as $\mathcal{L}_{ov}^{ij}$, is the TOV of i if it selects node $j \in \Omega_i$ as its parent. Mathematically this can be calculated as

$$\mathcal{L}_{ov}^{ij} = \mathcal{T}_{ov}^{j} + p_{ov}^{ij} \tag{8}$$

The sink S broadcasts beacons with $\mathcal{T}_{ov}^{S} = 0$. For each entry j in its `NTable`, a node i calculates the minimum transmit power t_{ij} required to achieve a desired link quality Υ from the prediction model (using (7)) if the non-default (a, b) exists. Otherwise it considers its current transmit power level t_c. It then calculates its p_{ov}^{ij}, which is the POV corresponding to the transmit power (t_{ij} or t_c) and records the metric $\mathcal{L}_{ov}^{ij}$ which is the sum of that p_{ov}^{ij} and the $\mathcal{T}_{ov}^{j}$ sent by neighbor j. It also calculates the ℓ_{ij} and $\wp_{ij}$ based on that transmit power (t_{ij} or t_c). It then chooses the entry corresponding to the minimum $\mathcal{L}_{ov}^{ij}$ $\forall$ $j \in \Omega_i$ such that:

(i) node-ETX of i is less than that of j, i.e. $\zeta_i < \zeta_j$
(ii) link $i \rightarrow j$ has a reasonable link-ETX, i.e. $\ell_{ij} < \frac{1}{\Upsilon}$[3]

[3] As the link-ETX and link quality (or PDR) are the inverse of each others.

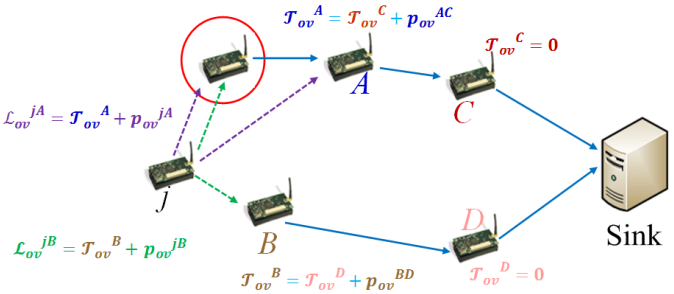

FIGURE 10: Illustration of the proposed PCOR scheme.

(iii) the path-ETX through j is less than (τ + min-ETX), i.e. $\wp_{ij} < \tau + \lambda_i$, where τ is a predefined threshold

Condition(i)-(ii) avoids routing loop and also avoids the links with very poor quality. Condition(iii) ensures that the routes with qualities significantly lower than the best quality route are avoided.

The $\mathcal{T}_{ov}^{i}$ is then calculated as:

$$\mathcal{T}_{ov}^{i} = \min_{\forall j \in \Omega_i} \mathcal{L}_{ov}^{ij} \quad \text{s.t. (i)-(iii)} = \mathcal{L}_{ov}^{lj} \text{ (assume)} \tag{9}$$

where $l \in \Omega_i$ is chosen as the parent of i. The metric $\mathcal{T}_{ov}^{i}$ is then broadcasted by i using the beacon messages. In case of a tie, i chooses the parent that gives the least path-ETX. The intuition behind this is that (a) the route with minimum TOV is the route that has the minimum overhearing impact on the critical nodes, and (b) the route with minimum path-ETX gives the route with minimum cost. While choosing its parent l in this process, the node i determines its transmit power (t_{il} or t_c) as well. This fulfills our twin objectives of *joint* power control and route adaptation to avoid overhearing on the critical nodes. This transmit power and parent selection process are carried on periodically.

The entire parent selection phase at a node i is discussed in line 1-15 of Algorithm 1. In Algorithm 1 the neighbors that fulfills conditions (i)-(iii) are stored in a list denoted as Γ_i (line 10-11). Then the neighbor $l \in \Omega_i$ that has the minimum LOV is chosen as the parent (line 12-13). PCOR does not incur any additional control overhead other than periodic beacon updates. Issues such as routing loop detection and repairing are tackled similar to CTP.

C. AN ILLUSTRATIVE EXAMPLE

Fig. 10 shows an example of our PCOR scheme. The critical node is shown within the red circle. Assume that A, B, and j are the neighbors of the critical node. As the sink is not in the neighboring region of the critical node, it broadcasts $\mathcal{T}_{ov}^{S}$ = 0. Similarly as C and D are not in the neighboring region of the critical node, they also broadcast $\mathcal{T}_{ov}^{C}$ and $\mathcal{T}_{ov}^{D}$ as zero. Next as A, B, and j are the neighbors of the critical node, assume that they want to reduce their power. Thus A and B determine their corresponding minimum transmit power level to maintain the required link-quality, correspondingly calculate their TOVs and broadcast. Now j needs to choose its parent in between A and B. So it first checks t_{jA} with

This article has been accepted for publication in a future issue of this journal, but has not been fully edited. Content may change prior to final publication. Citation information: DOI 10.1109/ACCESS.2019.2937894, IEEE Access

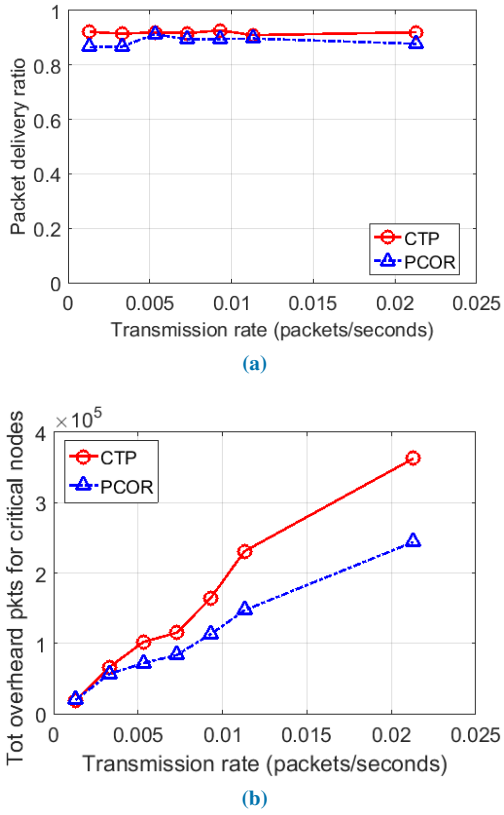

FIGURE 11: Comparison of PCOR vs CTP. The variation of (a) packet delivery ratio and (b) packets overheard by the critical nodes with different rates.

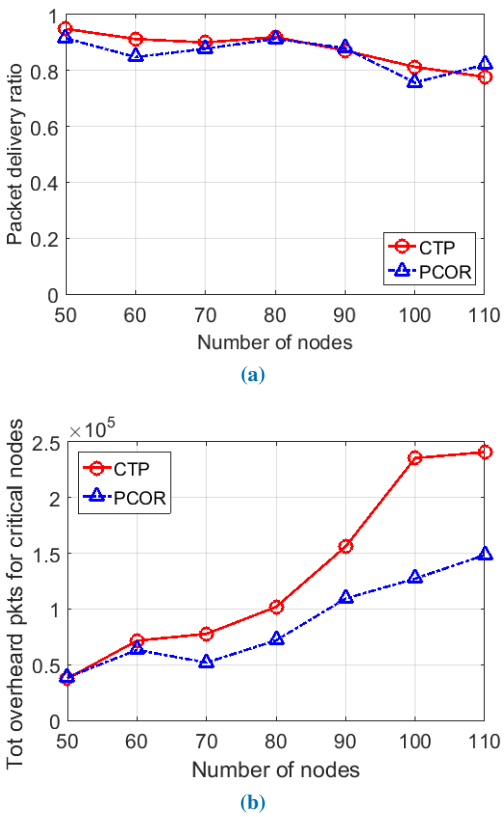

FIGURE 12: Comparison of PCOR vs CTP. The variation of (a) packet delivery ratio and (b) packets overheard by the critical nodes with different node densities.

which it needs to transmit to maintain a link-quality, and correspondingly calculate p_{ov}^{jA} and $\mathcal{L}_{ov}^{jA}$. It similarly determines t_{jB} and calculates the corresponding p_{ov}^{jB}. If $\mathcal{L}_{ov}^{jB} < \mathcal{L}_{ov}^{jA}$, it chooses B as its parent as well as its transmit power t_{jB}. Otherwise it chooses A as its parent with the corresponding transmit power. Thus the parent selection is done jointly with the power control in PCOR.

VII. PERFORMANCE EVALUATION

We now present the performance evaluations of PCOR obtained from computer simulations as well as using experimental testbeds. Simulation experiments were conducted by implementing PCOR in Castalia [61], which is an application level WSN simulator built on OMNET++. The experimental testbeds were developed using MICAz sensor nodes. We obtain performance results that depict (a) the reduction of overhearing at designated critical nodes achieved by PCOR in comparison to a purely link-quality based routing protocol, i.e. CTP, and (b) the corresponding packet delivery ratios, obtained under identical network conditions. Note that PCOR is developed with the objective of reducing overhearing effects on the sensor nodes that are energy critical, which has not been addressed in other power control and routing schemes that were reported in literature, such as [48], [49], [52]. Hence, we chose to evaluate the performance improvement of PCOR with respect to CTP only and not any other scheme.

We program the *LowPowerListening (LPL)* scheme [8] with a sleep interval of 125 milliseconds, i.e. nodes wake up 8 times in a second to sense the channel. According to LPL, a preamble that spans the duration of a wake-up interval, i.e. ∼125 milliseconds, was assumed for all cases. We experimentally recorded the current consumption of all the events, which are listed in Table 2[4]. The current consumption in different power levels ranging from 0 dBm to -25 dBm are also shown in Table 2. These values are used in our simulations in the next subsections.

A. SIMULATION RESULTS

We simulate a WSN where the sensor nodes are placed in a uniform grid over an area of 100×100 sq. meter. We assume that 10% of the nodes are energy-critical, i.e. receive poor sunlight and thus have less energy availability compared to others. The beacon interval is varied in between 5 seconds to 50 seconds similar to *Trickle* algorithm [62] used in CTP. The purpose of using *Trickle* is to adapt the beacon exchanges depending on the network stability. The maximum number of retransmissions is set to 3. For our performance evaluations

[4]Note that the manufacturer's datasheet reports the current consumption of a MICAz mote at 0 dBm to be 17.4 mA and 19.7 mA in transmit and receive modes, respectively [16]. However, for our performance evaluations we assume the measured values of 20 mA for these two modes, which is a close approximation.

This article has been accepted for publication in a future issue of this journal, but has not been fully edited. Content may change prior to final publication. Citation information: DOI 10.1109/ACCESS.2019.2937894, IEEE Access

TABLE 2: Different Parameters for MICAz

Var	Values	Var	Values	Var	Values	Var	Values
I_{Br}	20 mA	T_{Br}	140 ms	I_{Dr}	20 mA	T_{Dr}	140 ms
I_P	20 mA	T_P	3 ms	I_S	7.5 mA	T_S	112 ms

Var	Values	Var	Values
I_{Bt}, I_{Dt}	17.4 mA (0 dBm), 16.5 mA (-1 dBm) 15.2 mA (-3 dBm), 13.9 mA (-5 dBm) 12.5 mA (-7 dBm), 11.2 mA (-10 dBm) 9.9 mA (-15 dBm), 8.5 mA (-25 dBm)	T_{Bt}, T_{Dt}	140 ms

we assume τ to be 0.5. Routes are updated in every 8 seconds. Initially the nodes adapt their transmit power (if necessary) periodically in every 5 minutes. When a node obtains enough confidence for using the prediction model, it adapts its transmit power in conjunction with the route adaptation. Each simulation is run for around four hours.

Performance under variable transmission rates: Fig. 11 shows the overall packet delivery ratio and the total number of packets overheard by the critical nodes in a network of 80 nodes, with varying transmission rate. It can be observed that the packet delivery ratio is above 90% for all cases. However, PCOR reduces the total overhearing at the critical nodes upto 25% as compared to CTP. This clearly shows that PCOR is effective in reducing overhearing on the energy-critical nodes, without significantly affecting the overall packet delivery ratio. The improvement is marginal for low transmission rate, because the POC remains low in such cases. We can also observe that the overhearing increases almost linearly with increasing transmission rates.

Performance under varying node density: Fig. 12 shows the performance of PCOR and CTP with varying node densities. Here, we vary the number of nodes from 50 to 110 within the same geographic area. The packet transmission rate is set to 0.005 packets/secs for all nodes. It is observed that with varying node densities, PCOR reduces the overhearing effects by upto ∼40% as compared to CTP. We can also observe that with low node-density the improvement is marginal. This is because with low node-density, the sensor nodes have lesser number of neighbors to de-route the traffic and at the same time have lesser chances of joint power adaptation and routing. The POC also reduces with lesser node-density.

B. EXPERIMENTAL RESULTS

Observation of power control and route adaptation: To observe the impact of PCOR on transmission power levels of neighbors of a critical node and associated route adaptations, we first developed an experimental testbed comprising of 13 MICAz motes which were deployed in an area of 12 × 9 meters^2. The experiment was conducted in a laboratory environment, cluttered with computing equipment, furniture, and electronics machinery. The transmit power of the sensor nodes are varied in between -13 dBm (corresponds to the power level of 9 for MICAZ motes) and -28.5 dBm (corresponding power level is 2). Also $\mathcal{E}^m$ and $\mathcal{E}^M$ are assumed to be 2.5 and 3 respectively. The beacon and data packet transmission intervals are assumed to be 10 and 15 seconds respectively.

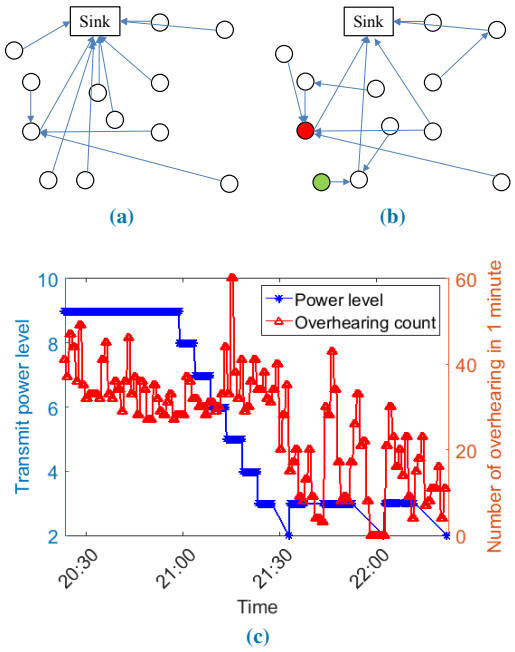

FIGURE 13: An instance of our network topology (a) before and (b) after changing the battery capacity of the critical node. The red node is made to be a critical node after 25 minutes. (c) Overhearing of the critical node (shown in red), and the transmit power of a neighbor (shown in green) of the critical node.

Fig 13(a) depicts the layout of the sensor nodes used in the experiment. The experiment was started with all nodes at 100% battery capacity, i.e. 3.0V. After 25 minutes, the battery voltage of the node marked in red is manually reduced to 50% of its operating range using a variable power source, to emulate a critical node. Fig 13 shows one instance of the data gathering tree of our network before and after changing the capacity of the critical node. This figure shows that when all nodes are in good state of battery, all of them directly send their traffics to the sink as all of them are in their highest power level. Later on when the energy level of the red node become critical, nodes started reducing their transmit power and start multi-hopping to forward packets to the sink. Fig 13(c) shows the corresponding reductions of the transmit power level of a neighboring node, marked in green, and the corresponding effect on overhearing at the critical node with time. This is because of the fact that other neighboring nodes started reducing their transmit power to avoid overhear the critical node. This short experiment clearly shows the effectiveness of our proposed scheme in reducing overhearing on the critical node.

Impact on overhearing and packet delivery ratio with multiple critical nodes: To evaluate the performance of PCOR in a larger network involving multiple critical nodes, we

This article has been accepted for publication in a future issue of this journal, but has not been fully edited. Content may change prior to final publication. Citation information: DOI 10.1109/ACCESS.2019.2937894, IEEE Access

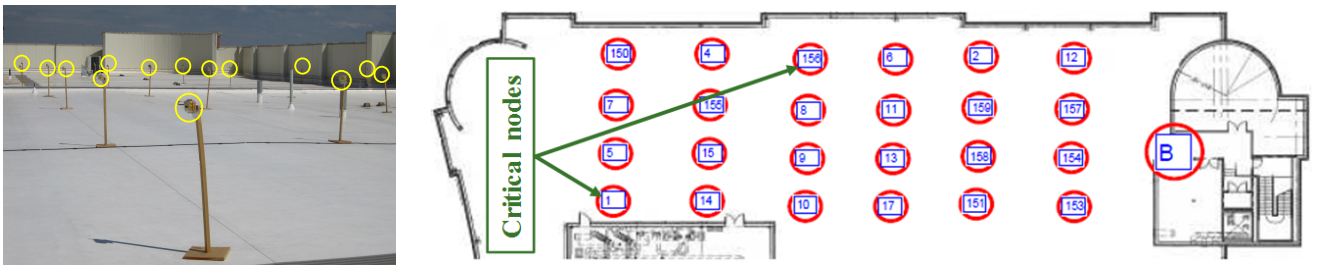

FIGURE 14: (a) A 25-node wireless sensor network testbed. (b) The map of the wireless sensor network testbed. Node 1 and Node 156 are made to be resource critical nodes. "B" denotes the sink node.

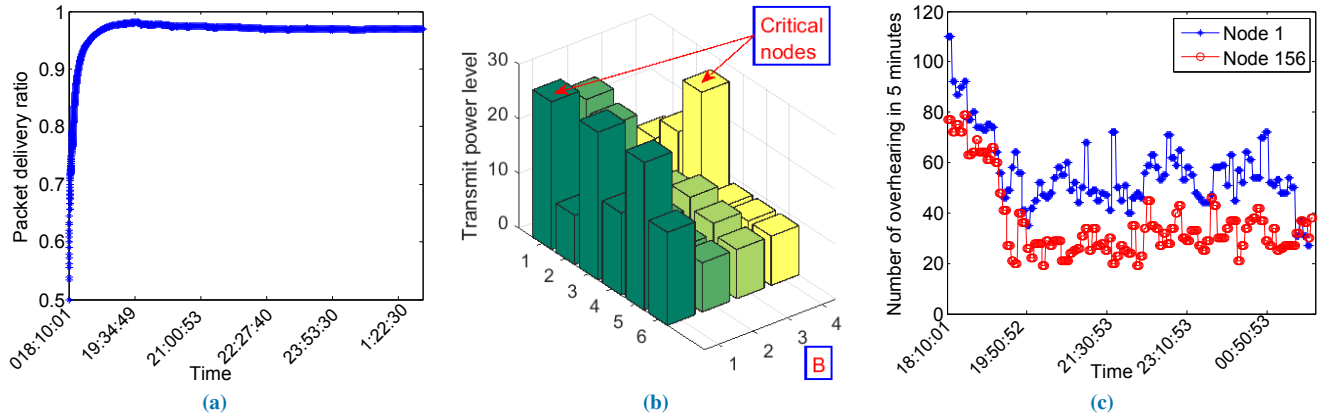

FIGURE 15: (a) Overall packet delivery ratio to the sink over time. (b) Transmit power levels of different nodes, power level 27 corresponds to -1 dBm and power level 9 corresponds to -13.4 dBm. (c) Number of packets overheard by the two critical nodes over time.

developed an experimental testbed consisting of 25 MICAz sensor nodes that was deployed on the roof of an academic building at UNC Charlotte. The nodes were programmed with PCOR using TinyOS [63] and placed at locations as indicated in Fig. 14. At initiation, the sensor nodes build the data collection tree to forward their sensed data to the sink node. The beacon interval is adaptively varied between 525 milliseconds and 1 minute, i.e. each node starts sending its beacon at an interval of 525 milliseconds and then progressively increases the sending interval until it reaches 10 seconds to conserve energy and bandwidth. The occurrence of specific events such as the detection of routing loops triggers a reset of the sending interval. Such resets are necessary in order to make the scheme able to quickly react to topology or environmental changes. The nodes send data packets with an interval of 1 minute. To execute the experiment within the limited deployment area, the transmit power is varied between -1 dBm to -13.4 dBm (i.e. from power levels from 27 to 8). We place two critical nodes (nodes 1 and 156) whose energy availability is assumed to be significantly lower compared to others. The maximum number of retransmission limit is set to 5. The values of $\mathcal{E}^m$ and $\mathcal{E}^M$ are assumed to be 1.5 and 2 respectively.

Fig. 15(a)-(c) show the results that are obtained over a duration of six hours. After deployment the nodes initially use their maximum transmit power level of -1 dBm. As the critical-nodes announce their health-metrics and POCs, their non-critical neighbors gradually reduce their transmit power levels while all other nodes adapt their routes to avoid overhearing caused to the energy-critical nodes. Fig. 15(b) shows the transmit power levels of the sensor nodes six hours after the deployment. From Fig. 15(b) we can observe that that most of the sensor nodes significantly reduce their transmit power levels. Fig. 15(b) also shows some spatial variations in transmit power levels of the non-critical nodes. This happens due to their individual link characteristics in between the sensor nodes and their neighbors. Fig. 15(c) illustrates the variation of overhearing on the critical nodes over the period of six hours. Fig. 15(c) clearly shows that immediately after deployment the overhearing on the critical nodes are significantly high. However, the amount of overhearing at the critical nodes is reduced by up to 75% because of the network wide power control and route adaptations. These results demonstrate that PCOR significantly reduces energy wastage due to overhearing on the energy-critical nodes without affecting the packet delivery ratio significantly (Fig. 15(a)).

VIII. CONCLUSIONS

In this paper, we consider a tree-based, rechargeable WSN under data collection traffic with asynchronous duty-cycling.

The fundamental challenge of such networks is the spatio-temporal variability of the energy availability and consumption patterns of the individual nodes. Another important challenge is a significant amount of energy consumption due to overhearing which results in localized node outages. We propose a distributed joint power-control and routing protocol that reduces overhearing at nodes that are critically low in energy resources while maintaining reliable quality of multihop communications from all nodes to the sink. Through simulations and experimental tests using implementations on the WSN platform, we demonstrate that our proposed scheme reduces overhearing on the energy-critical nodes by upto 75% without compromising the overall packet delivery ratio. The proposed scheme does not incur any additional overhead other than periodic beacon updates, which makes it suitable for implementations in real-life rechargeable sensor networks to ensure their continuous and long-terms operations.

REFERENCES

[1] "Enocean," http://www.enocean.com/en/products-technology/.
[2] "Texas instruments ez430-rf2500-seh," http://www.ti.com/lit/ug/slau273d/slau273d.pdf.
[3] A. Pal, B. Soibam, and A. Nasipuri, "A distributed power control and routing scheme for rechargeable sensor networks," in Proc. IEEE Southeastcon, 2013, pp. 1–5.
[4] A. Pal and A. Nasipuri, "PCOR: A joint power control and routing scheme for rechargeable sensor networks," in Proc. IEEE WCNC, 2014, pp. 2230–2235.
[5] A. Pal, "Dynamic routing with cross-layer adaptations for multi-hop wireless networks," Ph.D. dissertation, Charlotte, NC, USA, 2013.
[6] A. Pal and A. Nasipuri, "Lifetime of asynchronous wireless sensor networks with multiple channels and power control," in Proc. IEEE WCNC, 2014, pp. 2874–2879.
[7] O. Gnawali, R. Fonseca, K. Jamieson, D. Moss, and P. Levis, "Collection tree protocol," in Proc. SenSys, 2009, pp. 1–14.
[8] D. Moss, J. Hui, and K. Klues, "Low Power Listening, Core Working Group, TEP 105."
[9] P. Basu and J. Redi, "Effect of overhearing transmissions on energy efficiency in dense sensor networks," in Proc. IPSN, 2004, pp. 196–204.
[10] W. Ye, J. S. Heidemann, and D. Estrin, "An energy-efficient mac protocol for wireless sensor networks," in Proc. INFOCOM, 2002.
[11] A. Pal and A. Nasipuri, "DRCS: A distributed routing and channel selection scheme for multi-channel wireless sensor networks," in Proc. IEEE PerSeNS, 2013, pp. 602–608.
[12] A. Pal and A. Nasipuri, "Distributed routing and channel selection for multi-channel wireless sensor networks," J. Sensor and Actuator Networks, vol. 6, no. 3, p. 10, 2017.
[13] D. Moss and P. Levis, "BoX-MACs: Exploiting Physical and Link Layer Boundaries in Low-Power Networking," Stanford University, Tech. Rep., 2008.
[14] R. Jurdak, P. Baldi, and C. V. Lopes, "Adaptive low power listening for wireless sensor networks," IEEE Trans. Mob. Comput., vol. 6, no. 8, pp. 988–1004, 2007.
[15] G. Anastasi, M. Conti, and M. D. Francesco, "Extending the lifetime of wireless sensor networks through adaptive sleep," IEEE Trans. Industrial Informatics, vol. 5, no. 3, pp. 351–365, 2009.
[16] "Micaz Datasheet," http://www.memsic.com/userfiles/files/Datasheets/WSN/micaz_datasheet-t.pdf.
[17] M. Kubisch, H. Karl, and A. Wolisz, "Distributed algorithms for transmission power control in wireless sensor networks," in Proc. IEEE WCNC, 2003.
[18] "2.4 ghz ieee 802.15.4 / zigbee-ready rf transceiver," http://www.ti.com/lit/ds/symlink/cc2420.pdf.
[19] "nrf52840 product specification v1.0," http://infocenter.nordicsemi.com/pdf/nRF52840_PS_v1.0.pdf.
[20] M. Chiang, P. Hande, T. Lan, and C. W. Tan, "Power control in wireless cellular networks, foundation and trends," Proc. Networking, vol. 2, no. 4, pp. 381–533, 2007.
[21] J. Zander, "Performance of optimum transmitter power control in cellular radio systems," IEEE Transactions on Vehicular Technology, vol. 41, no. 1, pp. 57–62, 1992.
[22] J. Zander, "Distributed cochannel interference control in cellular radio systems," IEEE Transactions on Vehicular Technology, vol. 41, no. 3, pp. 305–311, 1992.
[23] T.-H. Lee and J.-C. Lin, "A fully distributed power control algorithm for cellular mobile systems," IEEE Journal on Selected Areas in Communications, vol. 14, no. 4, pp. 692–697, 1996.
[24] Q. Wu, "Performance of optimum transmitter power control in cdma cellular mobile systems," IEEE Transactions on Vehicular Technology, vol. 48, no. 2, pp. 571–575, 1999.
[25] V. Kawadia and P. R. Kumar, "Principles and protocols for power control in wireless ad hoc networks," IEEE Journal on Selected Areas in Communications, vol. 23, no. 1, pp. 76–88, 2005.
[26] N. Nie, C. Comaniciu, and P. Agrawal, A Game Theoretic Approach to Interference Management in Cognitive Networks. New York, NY: Springer, 2007, pp. 199–219.
[27] M. Torrent-Moreno, J. Mittag, P. Santi, and H. Hartenstein, "Vehicle-to-vehicle communication: Fair transmit power control for safety-critical information," IEEE Transactions on Vehicular Technology, vol. 58, no. 7, pp. 3684–3703, 2009.
[28] M. Krunz, A. Muqattash, and S.-J. Lee, "Transmission power control in wireless ad hoc networks: challenges, solutions and open issues," IEEE Network, vol. 18, no. 5, pp. 8–14, 2004.
[29] V. G. Douros and G. C. Polyzos, "Review of some fundamental approaches for power control in wireless networks," Computer Communications, vol. 34, no. 13, pp. 1580–1592, 2011.
[30] R. Ramanathan and R. Rosales-Hain, "Topology control of multihop wireless networks using transmit power adjustment," in Proc. IEEE INFOCOM, 2000, pp. 404–413.
[31] R. Rajaraman, "Topology control and routing in ad hoc networks: a survey," SIGACT News, vol. 33, pp. 60–73, 2002.
[32] L. Li, J. Y. Halpern, P. Bahl, Y.-M. Wang, and R. Wattenhofer, "Analysis of a cone-based distributed topology control algorithm for wireless multi-hop networks," in Proc. ACM PODC, 2001, pp. 264–273.
[33] R. Wattenhofer, L. Li, P. Bahl, and Y. min Wang, "Distributed topology control for power efficient operation in multihop wireless ad hoc networks," in Proc. IEEE INFOCOM, 2001, pp. 1388–1397.
[34] S. Singh, M. Woo, and C. S. Raghavendra, "Power-aware routing in mobile ad hoc networks," in Proc. ACM MobiCom, 1998, pp. 181–190.
[35] S. Doshi, S. Bhandare, and T. X. Brown, "An on-demand minimum energy routing protocol for a wireless ad hoc network," SIGMOBILE Mob. Comput. Commun. Rev., vol. 6, pp. 50–66, 2002.
[36] S. Doshi and T. X. Brown, "Minimum energy routing schemes for a wireless ad hoc network," in Proc. IEEE INFOCOM, 2002.
[37] J.-H. Chang and L. Tassiulas, "Energy conserving routing in wireless ad hoc networks," in Proc. IEEE INFOCOM, 2000.
[38] B. Chen, K. Jamieson, H. Balakrishnan, and R. Morris, "Span: an energy-efficient coordination algorithm for topology maintenance in ad hoc wireless networks," Wirel. Netw., vol. 8, pp. 481–494, 2002.
[39] A. Cerpa and D. Estrin, "ASCENT: Adaptive self-configuring sensor networks topologies," in Proc. IEEE INFOCOM, 2004.
[40] X. Wang, G. Xing, Y. Zhang, C. Lu, R. Pless, and C. Gill, "Integrated coverage and connectivity configuration in wireless sensor networks," in Proc. SenSys, 2003, pp. 28–39.
[41] A. T. Hoang, Y.-C. Liang, and M. H. Islam, "Power control and channel allocation in cognitive radio networks with primary users' cooperation," IEEE Transactions on Mobile Computing, vol. 9, pp. 348–360, 2010.
[42] C. U. Saraydar, N. B. Mandayam, and D. J. Goodman, "Efficient power control via pricing in wireless data networks," IEEE Transactions on Communication, pp. 291–303, 2002.
[43] F. Meshkati, H. V. Poor, and S. C. Schwartz, "Energy-efficient resource allocation in wireless networks: An overview of game-theoretic approaches," IEEE Signal Processing Magazine, pp. 56–68, 2007.
[44] S. K. Jayaweera and T. Li, "Dynamic spectrum leasing in cognitive radio networks via primary-secondary user power control games," Trans. Wireless. Comm., vol. 8, pp. 3300–3310, 2009.
[45] R. Ramanathan and R. Hain, "Topology control of multihop wireless networks using transmit power adjustment," in Proc. INFOCOM, 2000, pp. 404–413.
[46] M. Kubisch, H. Karl, A. Wolisz, L. C. Zhong, and J. M. Rabaey, "Distributed algorithms for transmission power control in wireless sensor networks," in Proc. WCNC, 2003, pp. 558–563.

[47] T. A. ElBatt, S. V. Krishnamurthy, D. Connors, and S. K. Dao, "Power management for throughput enhancement in wireless ad-hoc networks," in Proc. ICC, 2000, pp. 1506–1513.
[48] D. Son, B. Krishnamachari, and J. S. Heidemann, "Experimental study of the effects of transmission power control and blacklisting in wireless sensor networks," in Proc. SECON, 2004, pp. 289–298.
[49] S. Lin, J. Zhang, G. Zhou, L. Gu, J. A. Stankovic, and T. He, "ATPC: adaptive transmission power control for wireless sensor networks," in Proc. SenSys, 2006, pp. 223–236.
[50] J. Jeong, D. Culler, and J.-H. Oh, "Empirical analysis of transmission power control algorithms for wireless sensor networks," in Proc. INSS, 2007, pp. 27–34.
[51] O. Chipara, Z. He, G. Xing, Q. Chen, X. Wang, C. Lu, J. A. Stankovic, and T. F. Abdelzaher, "Real-time power-aware routing in sensor networks," in Proc. IEEE IWQoS, 2006, pp. 83–92.
[52] Y. Fu, M. Sha, G. Hackmann, and C. Lu, "Practical control of transmission power for wireless sensor networks," in Proc. IEEE ICNP, 2012, pp. 1–10.
[53] M. Rostami, J. Gummeson, A. Kiaghadi, and D. Ganesan, "Polymorphic radios: a new design paradigm for ultra-low power communication," in Proc. ACM SIGCOMM, 2018, pp. 446–460.
[54] "Xmesh user manual, Crossbow technology," http://www.xbow.com/Products, 2007.
[55] "Harnessing the power of the sun for embedded sensor networks," http://engineering.ucla.edu/harnessing-the-power-of-the-sun-for-embedded-sensor-networks/, 2005.
[56] National Solar Radiation Database, National Renewable Energy Laboratory. [Online]. Available: www.nrel.gov/rredc/solar_data.html
[57] V. Rajendran, K. Obraczka, and J. J. Garcia-Luna-Aceves, "Energy-efficient, collision-free medium access control for wireless sensor networks," Wirel. Netw., vol. 12, pp. 63–78, 2006.
[58] W. Ye, J. Heidemann, and D. Estrin, "An energy-efficient MAC protocol for wireless sensor networks," in Proc. IEEE INFOCOM, 2002, pp. 1567–1576.
[59] D. Tian and N. D. Georganas, "A coverage-preserving node scheduling scheme for large wireless sensor networks," in Proc. ACM WSNA, 2002, pp. 32–41.
[60] M. Sichitiu, "Cross-layer scheduling for power efficiency in wireless sensor networks," in Proc. IEEE INFOCOM, 2004, pp. 1740–1750.
[61] "Castalia: A Simulator for WSN," http://castalia.npc.nicta.com.au/.
[62] P. Levis, N. Patel, D. E. Culler, and S. Shenker, "Trickle: A self-regulating algorithm for code propagation and maintenance in wireless sensor networks," in Proc. NSDI, 2004, pp. 15–28.
[63] P. Levis and D. Gay, TinyOS Programming, 1st ed. New York, NY, USA: Cambridge University Press, 2009.

AMITANGSHU PAL received the B.E. degree in computer science and engineering from Jadavpur University, in 2008, and the Ph.D. degree in electrical and computer engineering from The University of North Carolina at Charlotte, in 2013. He was a Postdoctoral Scholar with Temple University, where he is currently an Assistant Professor with the Computer and Information Science Department. He has published over 50 conferences and journal papers. His current research interests include wireless sensor networks, reconfigurable optical networks, smart health-care, cyber-physical systems, mobile and pervasive computing, and cellular networks.

ASIS NASIPURI received his B.Tech. (Honors) degree in Electronics and Electrical Communication Engineering from the Indian Institute of Technology at Kharagpur, India in 1987, and his MS and Ph.D. degrees in Electrical and Computer Engineering from the University of Massachusetts at Amherst in 1990 and 1993, respectively. He is currently a Professor and Chair of the Department of Electrical and Computer Engineering (ECE) at the University of North Carolina at Charlotte. Dr. Nasipuri served as the Graduate Program Director of ECE from 2006 - 2013, and the Associate Chair and Coordinator of Undergraduate Programs of ECE from 2013 - 2014. Prior to joining UNC Charlotte, Dr. Nasipuri was a visiting researcher at the University of Texas at San Antonio (1998 - 2000) and a member of the faculty of the Department of Electronics and Electrical Communication Engineering at the Indian Institute of Technology at Kharagpur (1993 - 1998).

Dr. Nasipuri's research interests include protocols and algorithms for multihop wireless networks, which includes mobile ad hoc networks, wireless sensor networks, and wireless mesh networks; experimental research on wireless sensor networks, inlcuding application development, energy management, and sustainability issues; and analysis and design of distributed, sequential, and non-parametric signal detection schemes. He has published over 60 peer-reviewed papers and research articles on his research, which has received over 4000 citations. He received multiple federal and industrial research grants to support his research. Dr. Nasipuri serves in organization committes of numerous international conferences and symposia, journal editorial board, and proposal review panels. He served as the General Chair of the 2012 ACM International Symposium of Mobile Ad Hoc Networking and Computing (MobiHoc).